JOURNAL OF MOLECULAR SPECTROSCOPY 158, 170–176 (1993)

Infrared Emission Spectroscopy of Bismuth Monohydride and Bismuth Monodeuteride

HARTMUT G. HEDDERICH AND PETER F. BERNATH[1,2]

Centre for Molecular Beams and Laser Chemistry, Department of Chemistry, University of Waterloo, Waterloo, Ontario, Canada N2L 3G1

The high-resolution infrared emission spectra of bismuth monohydride and bismuth monodeuteride have been observed by Fourier transform spectroscopy. Gaseous BiH and BiD were produced by the direct reaction of the metal with hydrogen and deuterium, respectively. About 120 lines with $v = 1 \rightarrow 0$ to $v = 3 \rightarrow 2$ for each isotopomer have been measured. Dunham coefficients, Y_{ij}, have been derived in separate fits for the two molecules. In addition all data have been used in a combined fit to yield the mass-reduced Dunham constants, U_{ij}.

INTRODUCTION

Since the early 1930s several electronic transitions of BiH and BiD have been observed in emission and in absorption (*1–10*). The magnetic hyperfine structure of the electronic bands of BiH has been the subject of detailed studies (*6, 7, 10*). In several publications the properties of BiH have been predicted by ab initio calculations (*11–14*). The infrared rovibration spectra of BiH and BiD were observed in absorption by diode laser spectroscopy (*15, 16*). Diode laser spectroscopy has the advantage of very high sensitivity, but the disadvantage that a single longitudinal mode of a diode laser has continuous coverage of only 1 cm^{-1} or less. In cases like BiH and BiD, molecules with rather large values for the rotational constant B (5.138 302 cm^{-1} for BiH and 2.589 741 cm^{-1} for BiD), the spectral coverage is too poor to obtain a large number of transitions. Fourier transform infrared emission spectroscopy is a very sensitive method to study high-temperature metal hydrides at long wavelengths, as recently shown in the case of BaH (*17*). Although infrared emission spectroscopy at shorter wavelengths (less than 5 μm, the InSb detector cut-off) is not uncommon, BaH and BiH are the first examples of metal hydrides observed in the mid-infrared region. In this publication we report the observation of the high-resolution infrared emission spectra of BiH and BiD.

From the $(6p\sigma)^2\ (6p\pi)^2$ configuration of BiH we expect an $X\,^3\Sigma^-$ ground state (BiH is isovalent with NH). However, BiH follows Hund's coupling case (c) so the $^3\Sigma_1^-$ and $^3\Sigma_0^-$ spin components are widely separated (4936 cm^{-1}) and give rise to the $A1$ and $X0^+$ states (*9, 10*). In the early publications these two states were called $A\,^1\Pi$ and $X\,^1\Sigma^+$ because a Hund's case (a) p complex has the same energy level pattern as a Hund's case (c) $^3\Sigma^-$ state. In this work we observed only the $X0^+$ state, and the $A1$ state was not detected.

[1] Also: Department of Chemistry, University of Arizona, Tucson, AZ 85721.

[2] Camille and Henry Dreyfus Teacher–Scholar.

0022-2852/93 $5.00

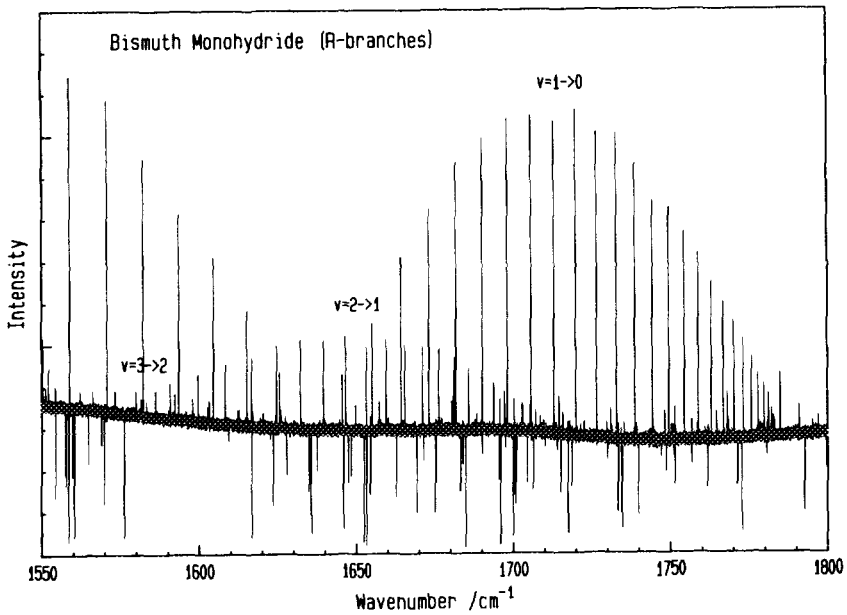

FIG. 1. Portion of the high-resolution infrared emission spectrum of BiH between 1500 and 1800 cm^{-1}. The spectrum shows the region of the R branches of $v = 1 \rightarrow 0$ to $v = 3 \rightarrow 2$. The absorption lines belong to H_2O.

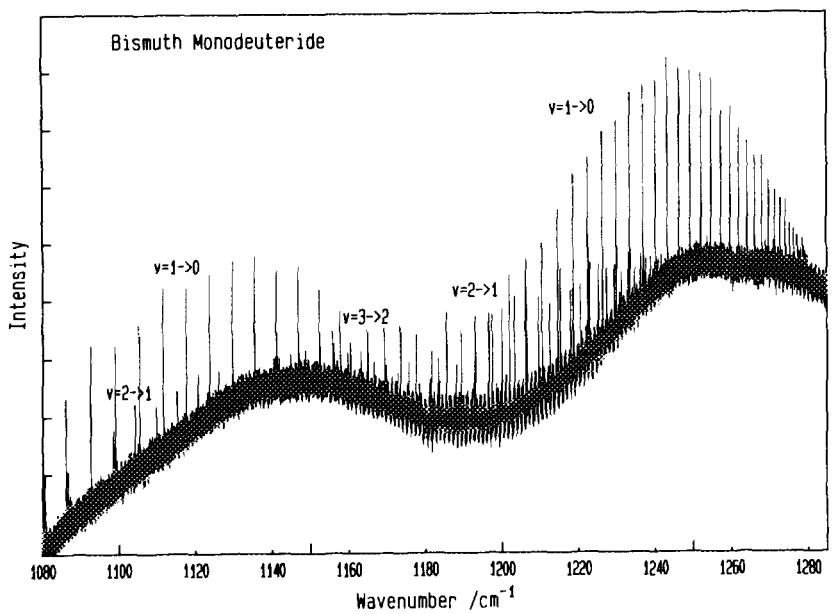

FIG. 2. Infrared emission spectrum of BiD. The fundamental band and the first and second hot bands in the R- and P-branch regions are indicated.

EXPERIMENTAL DETAILS

The high-resolution infrared emission spectra of BiH and BiD were observed with the Bruker IFS 120 HR Fourier transform spectrometer at the University of Waterloo. The resolution was 0.005 cm^{-1} with liquid-nitrogen-cooled HgCdTe detectors and a KBr beamsplitter. The spectral bandpass was limited to 1000–2200 cm^{-1} by an optical filter for the upper limit and by CaF_2 windows for the lower limit.

Gas-phase bismuth monohydride and bismuth monodeuteride molecules were produced in a tube furnace by the reaction of bismuth metal with hydrogen or deuterium. A 1-m-long stainless steel tube equipped with CaF_2 windows was used for all experiments. The tube was filled with about 50 g of Bi metal and pressurized with 20 Torr of hydrogen or deuterium and then heated to 1000°C.

TABLE I

Observed Line Positions of BiH (in cm^{-1})

J''	observed	o.–c.[a] $/10^{-5}$	J''	observed	o.–c. $/10^{-5}$	J''	observed	o.–c. $/10^{-5}$	J''	observed	o.–c. $/10^{-5}$
$v = 1 \rightarrow 0$			$v = 1 \rightarrow 0$			$v = 2 \rightarrow 1$			$v = 3 \rightarrow 2$		
$P(35)$	1136.2179[b]	293	$R(7)$	1705.69842	13	$P(10)$	1461.06122	−6	$P(13)$	1362.51841	−49
$P(34)$	1153.8445[b]	452	$R(8)$	1712.99248	4	$P(9)$	1473.37036	9	$P(12)$	1375.29545	11
$P(31)$	1205.7734[b]	389	$R(9)$	1719.95025	−3	$P(8)$	1485.42153	−9	$P(11)$	1387.82541	−5
$P(30)$	1222.7556[b]	202	$R(10)$	1726.56756	−3	$P(7)$	1497.21070	−19	$P(10)$	1400.10630	134
$P(29)$	1239.5725[b]	337	$R(11)$	1732.83999	−20	$P(6)$	1508.73327	−35	$P(9)$	1412.12919	−30
$P(28)$	1256.2137[b]	106	$R(12)$	1738.76369	−21	$P(5)$	1519.98513	−22	$P(8)$	1423.89550	80
$P(26)$	1288.96872	−11	$R(13)$	1744.33438	−20	$P(4)$	1530.96136	−26	$P(7)$	1435.39604	−17
$P(25)$	1305.07383	−10	$R(14)$	1749.54784	−27	$P(3)$	1541.65749	−47	$P(6)$	1446.63071	108
$P(24)$	1320.99166	−18	$R(15)$	1754.40020	−21	$P(2)$	1552.06961	−32	$P(5)$	1457.59090	35
$P(23)$	1336.71879	23	$R(16)$	1758.88718	−20	$R(0)$	1581.55489	−20	$P(4)$	1468.27390	−67
$P(22)$	1352.25014	11	$R(17)$	1763.00498	0	$R(1)$	1590.78465	−47	$P(3)$	1478.67960	235
$P(21)$	1367.58206	−5	$R(18)$	1766.74911	−6	$R(2)$	1599.70852	−11	$R(2)$	1534.93577	−204
$P(20)$	1382.71051	−9	$R(19)$	1770.11597	5	$R(3)$	1608.32110	−11	$R(3)$	1543.24792	50
$P(19)$	1397.63122	−4	$R(20)$	1773.10134	10	$R(4)$	1616.61846	−2	$R(4)$	1551.24095	59
$P(18)$	1412.33984	4	$R(21)$	1775.70131	20	$R(5)$	1624.59594	−14	$R(5)$	1558.91215	−10
$P(17)$	1426.83192	5	$R(22)$	1777.91175	19	$R(6)$	1632.24967	1	$R(6)$	1566.25889	20
$P(16)$	1441.10311	1	$R(23)$	1779.72870	9	$R(7)$	1639.57490	3	$R(7)$	1573.27543	15
$P(15)$	1455.14898	−8	$R(24)$	1781.14809	−19	$R(8)$	1646.56735	−6	$R(8)$	1579.95854	90
$P(14)$	1468.96525	−7	$R(25)$	1782.16523	−137	$R(9)$	1653.22318	23	$R(9)$	1586.30127	−11
$P(13)$	1482.54732	−10	$R(26)$	1782.77467	−493	$R(10)$	1659.53727	7	$R(10)$	1592.30263	51
$P(12)$	1495.89080	−6	$R(27)$	1782.9792[b]	−409	$R(11)$	1665.50591	3	$R(11)$	1597.95574	28
$P(11)$	1508.99110	−4	$R(28)$	1782.7693[b]	−438	$R(12)$	1671.12474	2	$R(12)$	1603.25685	−16
$P(10)$	1521.84372	−3	$R(29)$	1782.1394[b]	−738	$R(13)$	1676.38939	−5	$R(13)$	1608.20195	−41
$P(8)$	1546.78784	1	$v = 2 \rightarrow 1$			$R(14)$	1681.29579	1	$R(14)$	1612.78602	−108
$P(7)$	1558.87024	−1	$P(24)$	1264.12287	−120	$R(15)$	1685.83941	−9	$R(15)$	1617.00680	0
$P(6)$	1570.68695	8	$P(23)$	1279.58691	28	$R(16)$	1690.01630	−3	$v = 4 \rightarrow 3$		
$P(5)$	1582.23330	13	$P(22)$	1294.85034	−34	$R(17)$	1693.82201	−2	$R(2)$	1469.8382[b]	419
$P(4)$	1593.50471	8	$P(21)$	1309.91184	−50	$R(18)$	1697.25239	6	$R(3)$	1477.8347[b]	−111
$P(3)$	1604.49688	14	$P(20)$	1324.76769	2	$R(19)$	1700.30305	8	$R(4)$	1485.5188[b]	10
$P(2)$	1615.20518	18	$P(19)$	1339.41265	−1	$R(20)$	1702.96946	−22	$R(5)$	1492.8775[b]	−73
$P(1)$	1625.62496	4	$P(18)$	1353.84366	44	$R(21)$	1705.24834	17	$R(6)$	1499.9088[b]	−117
$R(0)$	1645.58185	−6	$P(17)$	1368.05551	30	$R(22)$	1707.13443	31	$R(8)$	1512.9728[b]	57
$R(1)$	1655.11032	24	$P(16)$	1382.04463	19	$R(26)$	1710.6657[b]	10	$R(9)$	1518.9936[b]	−21
$R(2)$	1664.33244	28	$P(15)$	1395.80718	53	$R(27)$	1710.5232[b]	−14	$R(11)$	1529.9943[b]	−111
$R(3)$	1673.24394	19	$P(14)$	1409.33768	12	$v = 3 \rightarrow 2$			$R(12)$	1534.9624[b]	−400
$R(4)$	1681.84072	23	$P(13)$	1422.63305	20	$P(16)$	1322.75350	−75			
$R(5)$	1690.11819	16	$P(12)$	1435.68829	13	$P(15)$	1336.24425	11			
$R(6)$	1698.07218	12	$P(11)$	1448.49891	−19	$P(14)$	1349.50149	107			

[a] observed minus calculated line positions using the mass-reduced Dunham constants of Table IV.

[b] absorption lines from Urban *et al.* *(16)*, diode laser spectroscopy.

TABLE II

Observed Line Positions of BiD (in cm^{-1})

J''	observed	o.–c.[a] $/10^{-5}$	J''	observed	o.–c. $/10^{-5}$	J''	observed	o.–c. $/10^{-5}$	J''	observed	o.–c. $/10^{-5}$
$v = 1 \rightarrow 0$			$v = 1 \rightarrow 0$			$v = 2 \rightarrow 1$			$v = 2 \rightarrow 1$		
$P(25)$	1016.35987	−121	$R(7)$	1210.44929	−40	$P(15)$	1055.50977	205	$R(21)$	1222.92497	−129
$P(24)$	1023.68773	−5	$R(8)$	1214.58014	−9	$P(14)$	1061.89508	134	$R(22)$	1225.22366	−101
$P(23)$	1030.93471	−138	$R(9)$	1218.59475	15	$P(13)$	1068.19045	79	$R(23)$	1227.38965	−212
$P(22)$	1038.10527	40	$R(10)$	1222.49141	−28	$P(12)$	1074.39454	22	$R(24)$	1229.42438	−212
$P(21)$	1045.19336	38	$R(11)$	1226.27043	2	$P(11)$	1080.50645	−14	$R(25)$	1231.32379	−401
$P(20)$	1052.19939	12	$R(12)$	1229.92976	7	$P(10)$	1086.52558	28	$R(26)$	1233.09213	−248
$P(19)$	1059.12233	−24	$R(13)$	1233.46863	18	$P(8)$	1098.27769	23	$R(27)$	1234.72265	−324
$P(18)$	1065.96167	−8	$R(14)$	1236.88574	13	$P(7)$	1104.01013	152	$R(28)$	1236.21651	−408
$P(17)$	1072.71554	−10	$R(15)$	1240.18017	7	$P(6)$	1109.64245	84	$R(29)$	1237.57334	−430
$P(16)$	1079.38328	20	$R(16)$	1243.35076	−12	$P(5)$	1115.17673	142	$R(30)$	1238.79191	−408
$P(15)$	1085.96312	22	$R(17)$	1246.39703	16	$P(4)$	1120.61041	184	$R(32)$	1240.81057	−184
$P(14)$	1092.45260	−134	$R(18)$	1249.31745	43	$P(3)$	1125.94191	166	$R(33)$	1241.60528	−308
$P(13)$	1098.85525	21	$R(19)$	1252.11101	71	$P(2)$	1131.16842	−76	$v = 3 \rightarrow 2$		
$P(12)$	1105.16494	−10	$R(20)$	1254.77564	−1	$R(2)$	1155.73612	302	$R(4)$	1132.21324	13
$P(11)$	1111.38253	−23	$R(21)$	1257.31207	2	$R(3)$	1160.32196	16	$R(7)$	1144.65015	5
$P(10)$	1117.50632	−72	$R(22)$	1259.71926	81	$R(4)$	1164.80030	45	$R(8)$	1148.56869	204
$P(9)$	1123.53629	−44	$R(23)$	1261.99455	72	$R(5)$	1169.16705	93	$R(9)$	1152.36660	−19
$P(8)$	1129.47028	−36	$R(24)$	1264.13740	22	$R(6)$	1173.41998	47	$R(10)$	1156.04888	−53
$P(7)$	1135.30733	−31	$R(25)$	1266.14807	61	$R(7)$	1177.55920	31	$R(11)$	1159.61452	111
$P(6)$	1141.04593	−61	$R(26)$	1268.02505	138	$R(8)$	1181.58354	37	$R(12)$	1163.05689	−78
$P(5)$	1146.68556	−65	$R(27)$	1269.76636	157	$R(9)$	1185.49244	121	$R(13)$	1166.38054	−56
$P(4)$	1152.22406	−142	$R(28)$	1271.37153	171	$R(10)$	1189.28241	43	$R(14)$	1169.58244	−15
$P(3)$	1157.66298	−22	$R(29)$	1272.83936	160	$R(11)$	1192.95525	94	$R(15)$	1172.66103	−2
$P(2)$	1162.99796	−25	$R(30)$	1274.16973	213	$R(12)$	1196.50780	65	$R(16)$	1175.61622	85
$P(1)$	1168.22720	−219	$R(31)$	1275.35938	104	$R(13)$	1199.93966	28	$R(17)$	1178.44547	101
$R(0)$	1178.37809	246	$R(32)$	1276.40983	83	$R(14)$	1203.25003	9	$R(18)$	1181.14521	−201
$R(1)$	1183.29216	373	$R(33)$	1277.31839	−19	$R(15)$	1206.43749	−24	$R(19)$	1183.72232	−25
$R(2)$	1188.09191	−92	$R(34)$	1278.08722	112	$R(16)$	1209.50140	−29	$R(20)$	1186.16699	−241
$R(3)$	1192.78682	−90	$R(35)$	1278.71080	25	$R(17)$	1212.44039	−33	$R(21)$	1188.48711	49
$R(4)$	1197.37150	−46	$R(36)$	1279.19204	107	$R(18)$	1215.25305	−71	$R(22)$	1190.67182	−132
$R(5)$	1201.84440	−4	$R(37)$	1279.52610	−26	$R(19)$	1217.93866	−109	$R(23)$	1192.72773	−14
$R(6)$	1206.20396	−10				$R(20)$	1220.49625	−135			

[a] *observed minus calculated line positions using the mass-reduced Dunham constants of Table IV.*

Absorption spectra were taken up to a temperature of 700°C. These spectra showed no features belonging to BiH or BiD. At a temperature of 700°C the light source (globar) was switched off and emission spectra were taken. At this temperature weak emission features around 1600 cm^{-1} (BiH) or 1200 cm^{-1} (BiD) were observed. The intensities of the bands increased with increasing temperature and showed a maximum at about 1000°C. Figures 1 and 2 show the rovibrational emission spectra of BiH and BiD observed at a temperature of 1000°C.

RESULTS

The spectral analysis program PC-DECOMP, developed by J. W. Brault, was used for data analysis. The line profiles were fit to Voigt lineshape functions. The signal-to-noise ratio for the strongest lines in the BiH and BiD spectra was about 40. The precision of the line positions is better than 0.0003 cm^{-1}, but several of the weaker lines were determined only to about ± 0.001 cm^{-1}. The absolute calibration for BiH was accomplished with some impurity H_2O (*18*) lines in the cell. The BiD lines were calibrated against the absolute positions of BiH lines which were also present in the BiD experiment.

TABLE III

Dunham Coefficients for BiH and BiD (in cm^{-1})

Coefficient	BiH	BiD
Y_{10}	1699.517 00(42)[a]	1205.422 57(34)
Y_{20}	−31.925 33(35)	−16.050 00(21)
Y_{30}	0.038 25(11)	0.013 017(37)
$10^3 Y_{40}$	−7.692(12)	−1.949 8[b]
Y_{01}	5.138 301 9(28)	2.589 741 0(45)
Y_{11}	−0.148 836 2(25)	−0.053 106 1(16)
$10^3 Y_{21}$	0.221 9(12)	0.397 3(78)
$10^3 Y_{31}$	−0.073 50(15)	−0.107 0(12)
$10^3 Y_{02}$	−0.186 022 8(81)	−0.475 93(13)
$10^6 Y_{12}$	1.163 5(70)	0.205 6(20)
$10^6 Y_{22}$	−0.174 3(23)	−0.020 78(36)
$10^9 Y_{03}$	2.346 4(69)	0.350(12)
$10^9 Y_{13}$	−0.184 0(73)	−0.023 1(16)
$10^9 Y_{23}$	−0.041 3(24)	−0.002 48[b]

[a] Errors quoted in parentheses are one standard deviation.

[b] Calculated using the isotope relationship (Eq.2) and fixed.

Bands with $v = 1 \rightarrow 0$ to $v = 3 \rightarrow 2$ for BiH and BiD were picked out using an interactive color Loomis–Wood program. Data reduction was made by using the well-known Dunham equation (*19*) for the energy levels,

$$T(v, J) = \sum_{ij} Y_{ij}\left(v + \frac{1}{2}\right)^i [J(J+1)]^j, \tag{1}$$

where v and J are the vibrational and rotational quantum numbers. The Dunham coefficients are isotope-dependent and vary approximately with powers of the reduced mass ratio μ/μ^*,

$$Y_{ij}^* = Y_{ij}\left(\frac{\mu}{\mu^*}\right)^{(i/2+j)}, \tag{2}$$

where the asterisk designates an isotopically substituted species. Table III gives the Dunham constants calculated in separate least-squares fits for BiH and BiD from our infrared data (Tables I and II) and BiH infrared data for $v = 4 \leftarrow 3$, as well as some high-J transitions for $v = 1 \leftarrow 0$ and $v = 2 \leftarrow 1$ by Urban *et al.* (*16*).

Finally, all infrared transitions of BiH and BiD were combined and fitted to the mass-reduced Dunham expression including Watson's correction due to the breakdown of the Born–Oppenheimer approximation (*20, 21*),

$$Y_{ij} = \mu^{-(i+2j)/2} U_{ij}\left[1 + \left(\frac{m_e}{m_{H/D}}\right)\Delta_{ij}^{H/D}\right], \tag{3}$$

where μ is the reduced mass, U_{ij} are the mass-independent parameters, $m_{H/D}$ are the atomic masses for hydrogen and deuterium, m_e is the electron mass, and Δ_{ij} are the mass scaling factors for the nuclei. The mass-independent Dunham constants are listed in Table IV.

TABLE IV

Mass-Reduced Dunham Coefficients for BiH/BiD (in cm^{-1})

Coefficient	value
U_{10}	1703.042 87(33)[a]
U_{20}	−32.028 89(26)
U_{30}	0.037 753(93)
$10^3\ U_{40}$	−7.675 1(97)
U_{01}	5.178 790 2(77)
U_{11}	−0.149 903 2(23)
$10^3\ U_{21}$	0.214 7(11)
$10^3\ U_{31}$	−0.072 78(15)
$10^3\ U_{02}$	−0.191 373(19)
$10^6\ U_{12}$	1.151 6(69)
$10^6\ U_{22}$	−0.168 1(23)
$10^9\ U_{03}$	2.363 4(73)
$10^9\ U_{13}$	−0.169 9(70)
$10^9\ U_{23}$	−0.047 9(23)
Δ_{10}	−1.069 56(36)
Δ_{20}	−0.598 5(67)
Δ_{01}	−8.918 2(28)
Δ_{11}	−5.077(15)
Δ_{02}	−40.73(15)

[a] Errors quoted in parentheses are one standard deviation.

The spectroscopic constants of Tables III and IV are similar to those reported previously by Urban *et al.* (*16*), but they are about an order of magnitude more precise. The increase in precision (and accuracy) is due to the more extensive data set provided by the increased spectral coverage and the higher precision possible with a Fourier transform spectrometer. Although infrared Fourier transform emission spectroscopy at long wavelengths is not as sensitive as diode laser spectroscopy, it is more sensitive than traditional absorption spectroscopy.

ACKNOWLEDGMENTS

This work was supported by the Phillips Laboratory/Propulsion Directorate, Edwards Air Force Base, CA, and the Natural Sciences and Engineering Research Council of Canada (NSERC). Acknowledgment is made to the Petroleum Research Fund, administered by the American Chemical Society, for partial support of this work. Some support was also provided by the URIF program. H.G.H. thanks the Deutsche Forschungsgemeinschaft for a postdoctoral scholarship.

RECEIVED: August 27, 1992

REFERENCES

1. A. HEIMER AND E. HULTHÉN, *Nature* **127,** 557 (1931).
2. E. HULTHÉN, *Nature* **129,** 56–57 (1932).
3. E. HULTHÉN AND A. HEIMER, *Nature* **129,** 399 (1932).
4. A. HEIMER, *Z. Phys.* **95,** 328–336 (1935).
5. A. HEIMER, *Z. Phys.* **103,** 621–626 (1936).
6. E. HULTHÉN AND H. NEUHAUS, *Phys. Rev.* **102,** 1415–1416 (1956).
7. H. NEUHAUS, *Z. Naturforsch. A* **21,** 2113–2114 (1966).

8. M. A. KHAN AND Z. M. KHAN, *Proc. Phys. Soc. London* **88,** 211–215 (1966).
9. B. LINDGREN AND G. NILSSON, *J. Mol. Spectrosc.* **55,** 407–419 (1975).
10. E. H. FINK, K. D. SETZER, D. A. RAMSAY, M. VERVLOET, AND J. M. BROWN, *J. Mol. Spectrosc.* **142,** 108–116 (1990).
11. K. BALASUBRAMANIAN, *Chem. Phys. Lett.* **114,** 201–204 (1985).
12. K. BALASUBRAMANIAN, *J. Mol. Spectrosc.* **115,** 258–268 (1986).
13. A. F. RAMOS, N. C. PYPER, AND A. G. MAKI, *Phys. Rev. A* **38,** 2729–2739 (1988).
14. M. DOLG, W. KÜCHLE, H. STOLL, H. PREUSS, AND P. SCHWERTFEGER, *Mol. Phys.* **74,** 1265–1285 (1991).
15. A. M. R. P. BOPEGEDERA, C. R. BRAZIER, AND P. F. BERNATH, *Chem. Phys. Lett.* **162,** 301–305 (1989).
16. R.-D. URBAN, P. POLOMSKY, AND H. JONES, *Chem. Phys. Lett.* **181,** 485–490 (1991).
17. K. A. WALKER, H. G. HEDDERICH, AND P. F. BERNATH, *Mol. Phys.*, in press.
18. R. A. TOTH, *J. Opt. Soc. Am. B* **8,** 2236–2255 (1991).
19. J. L. DUNHAM, *Phys. Rev.* **41,** 721–731 (1932).
20. J. K. G. WATSON, *J. Mol. Spectrosc.* **45,** 99–113 (1973).
21. J. K. G. WATSON, *J. Mol. Spectrosc.* **80,** 411–421 (1980).